

Analyse du potentiel des mesures GNSS-R pour le suivi des états des surfaces continentales

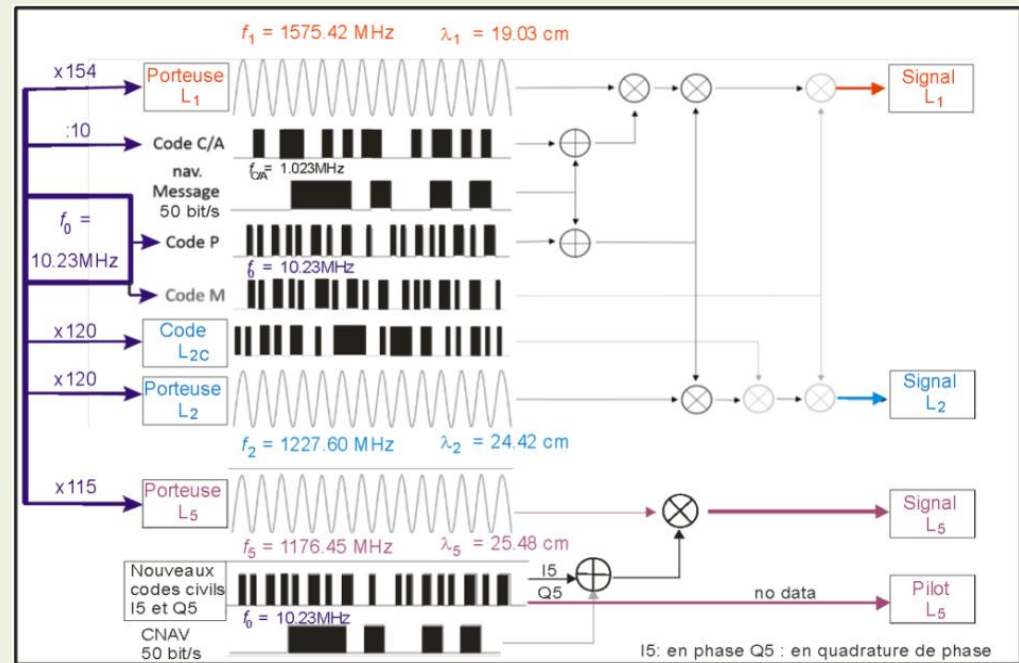
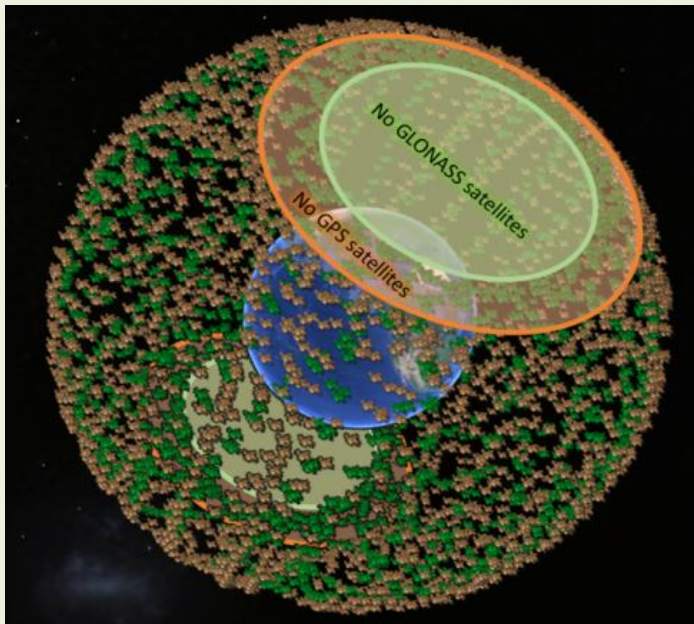
*Mehrez Zribi (CESBIO), Erwan Motte (CESBIO),
Pascal Fanise (CESBIO), Nicolas Baghdadi (TETIS),
Frédéric Baup (CESBIO), Sylvia Dayau (INRA),
Remy Fieuzal (CESBIO), Dominique Guyon (INRA),
Jean Pierre Wigneron (INRA)*



OUTLINE

- GNSS-R introduction
- GLORI instrument
- GLORI campaigns
- Results
- Conclusions

GNSS SATELLITE MEASUREMENTS



Here we can see the dense coverage of the two oldest GNSS constellations: the American GPS (orange) and the Soviet system GLONASS (green).

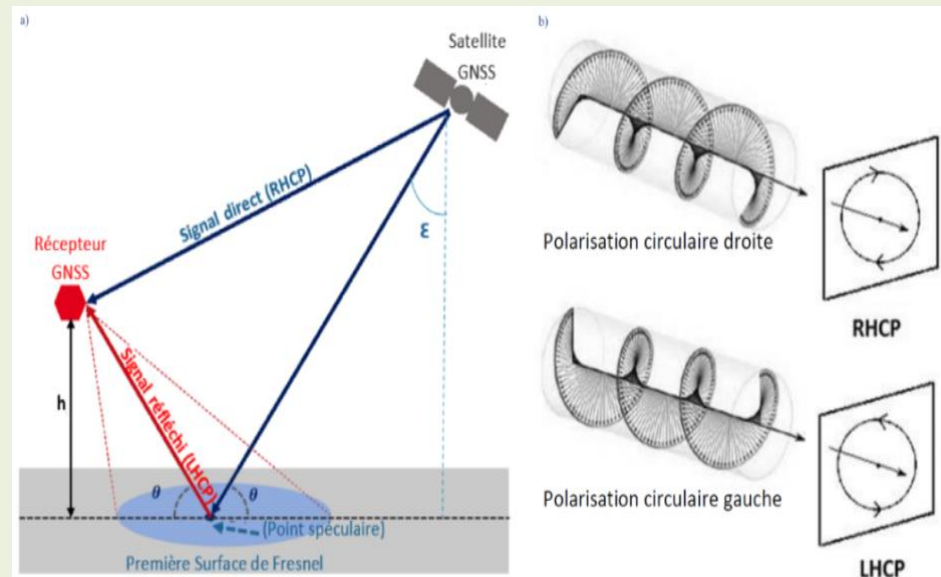
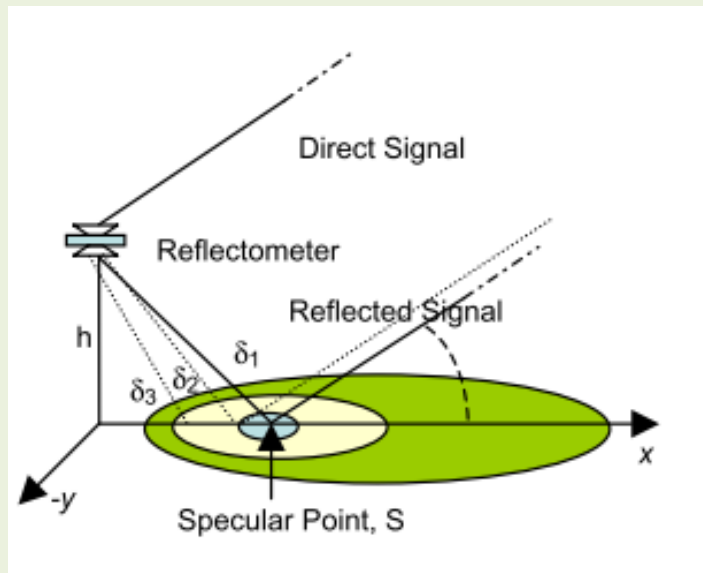
Structure of the GPS signal and improvements that have been made

WHAT POTENTIAL OF GNSS FOR GEOPHYSICAL MEASUREMENTS?

GNSS constellation	GPS (United States)	GLONASS (RUSSIA)	GALILEO (EUROPE)	BEIDOU2/COMPASS (CHINA)
Operational satellites	32 MEO	24 MEO	4 IOV → 30 MEO	5 → 27 MEO, 3 → 5 GEO and 3 IGSO
Altitude (km)	20 200	19 100	IOV: 23 222 MEO: 23 616	21 150
Orbital planes	6	3	3	3
Orbital period	11 h 58 min	11 h 15 min	14 h 21 min	12 h 53 min
Incline	55°	64.8°	56°	55°
Multiple access	CDMA	FDMA/CDMA A	CDMA	CDMA
Carriers and frequencies (MHz)	L1: 1575.42 L2: 1227.60 L5 : 1 176,45	L1: 1598.06 to 1605.38 L2: 1242.94 to 1248.63 L3: 1207.14 L5: 1176.45	E1: 1575.42 E5a: 1176.45 E5b : 1207.14 E6: 1278.75	B1: 1561.10 B1-2: 1589.74 B2: 1207.14 B3: 1268.52
Modulation	BPSK, BOC, TMBOC	BPSK, BOC	BPSK, BOC, CBOC, AltBOC	QPSK, BOC, MBOC, TMBOC
Statuts	OP	OP	VAL	~OP
OP: operational, ~OP: quasi operational, VAL: validation phase				
Code Division Multiple Access: CDMA, Frequency DMA: FDMA				

GNSS-R APPROACH

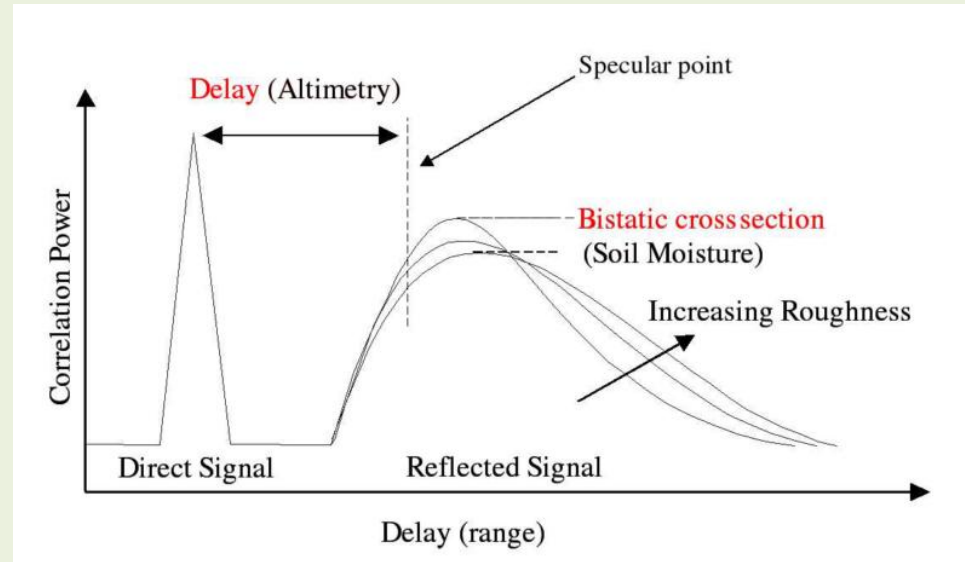
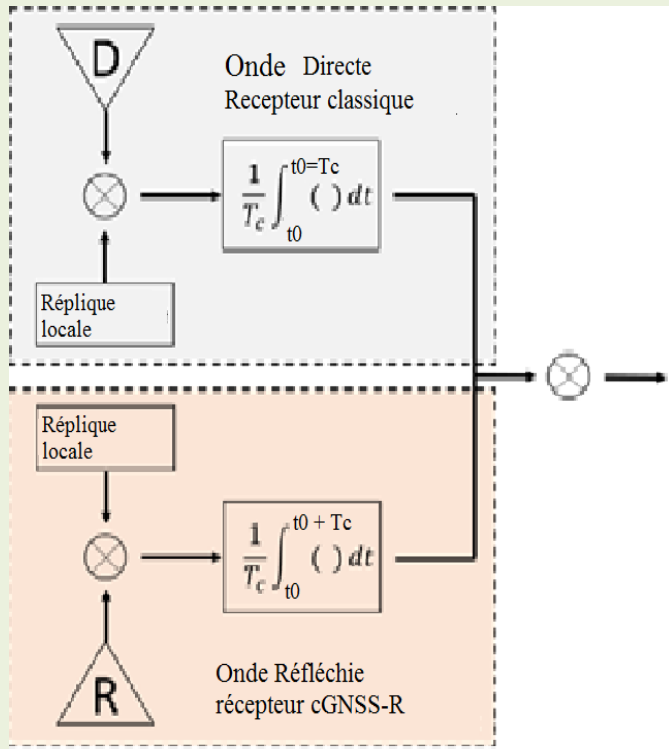
GNSS REFLECTOMETRY (GNSS-R: GLOBAL NAVIGATION SATELLITE SYSTEM - REFLECTOMETRY) IS A BISTATIC RADAR REMOTE SENSING TECHNOLOGY (TRANSMITTERS AND RECEIVERS ARE NOT IN THE SAME PLACE) THAT USES MICROWAVE SIGNALS OF OPPORTUNITY FROM RADIO NAVIGATION CONSTELLATIONS.



GNSS-R by waveform analysis technique: Each antenna pair corresponds to a channel that measures the direct signal with its up-looking antenna and another channel measuring the signal reflected by the surface with its down-looking antenna.

Interferometric Pattern Technique : Technique based on the coherent addition of direct and reflected GNSS signals on a antenna pointing to horizon.

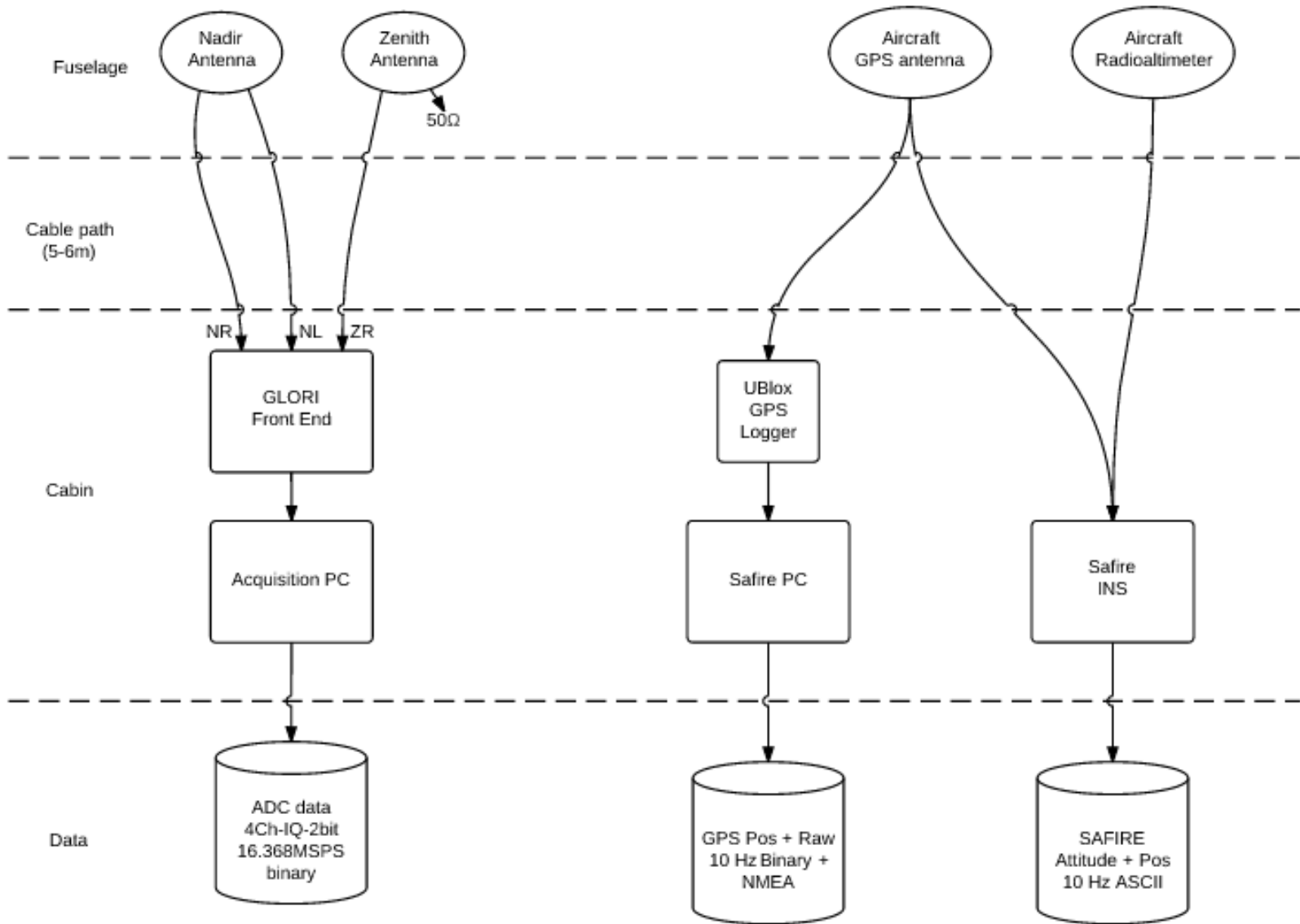
GNSS-R MEASUREMENT TECHNIQUES (WAVEFORM ANALYSIS)



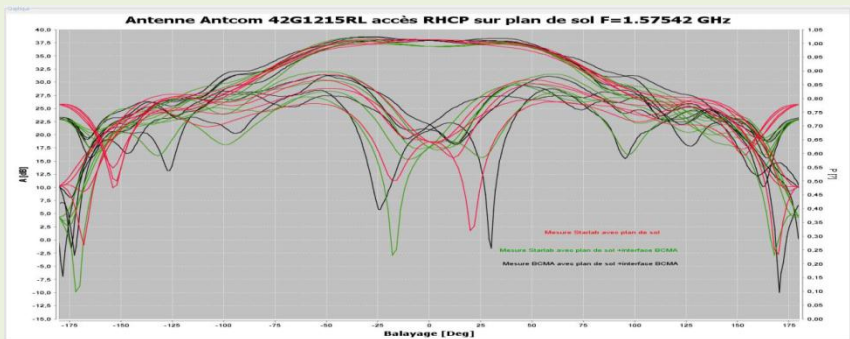
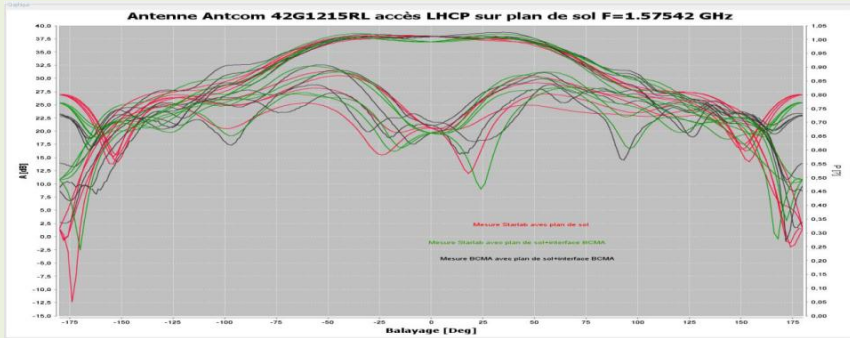
Cross-correlation of the received signal with replica of the code for different delays and Doppler shifts (Garrison et al., 1998)

$$Y^c(t_0, \tau, f_d) = \frac{1}{T_c} \int_{t_0}^{t_0+T_c} s_R(t) a^*(t-\tau) e^{-j2\pi(f_c + f_d)t} dt$$

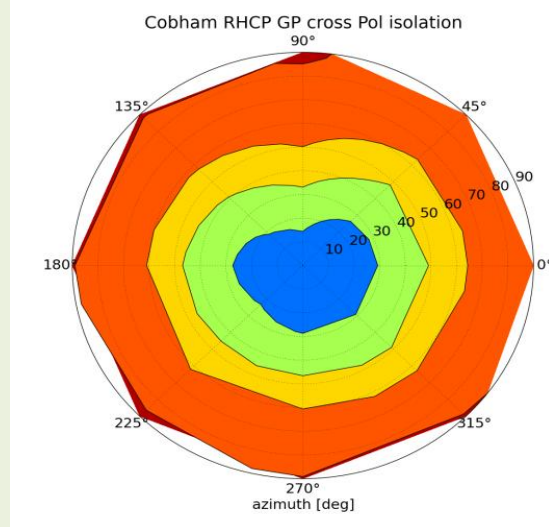
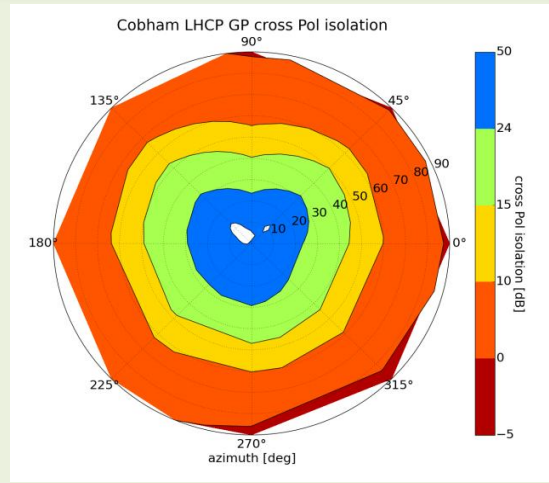
GLORI AIRBORNE INSTRUMENT



GLORI INSTRUMENT ANTENNAS

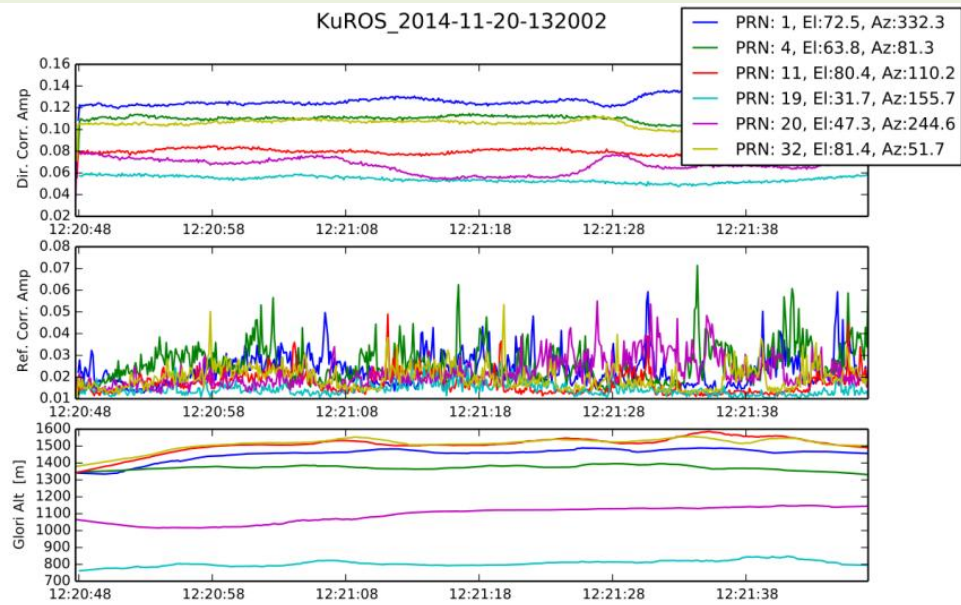
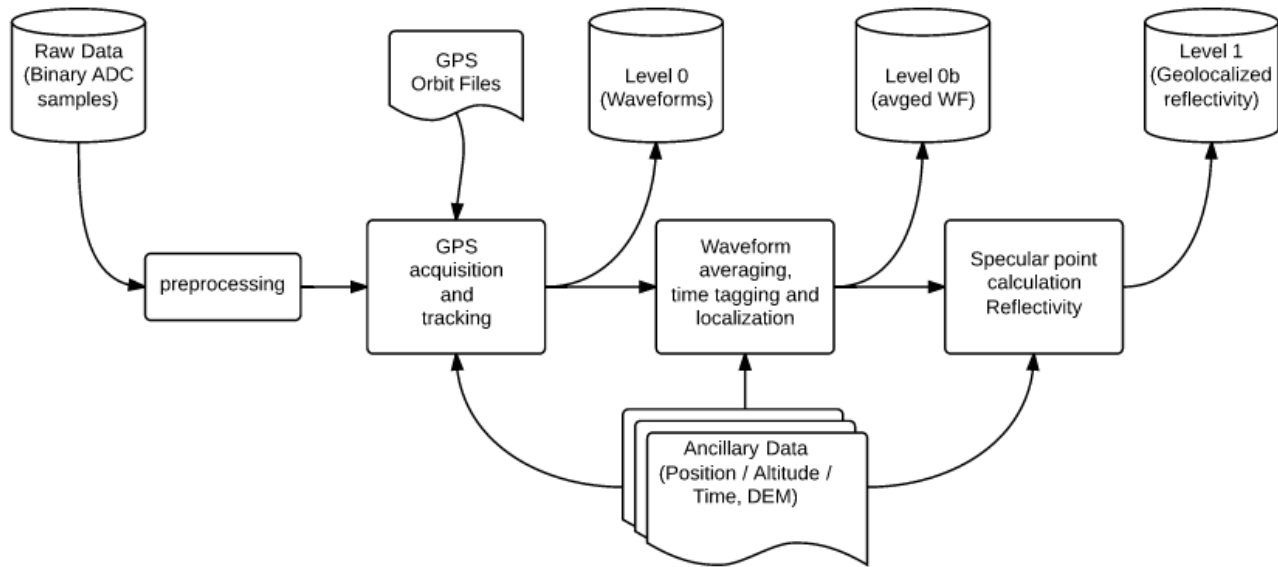


Radiation pattern of GLORI antennas



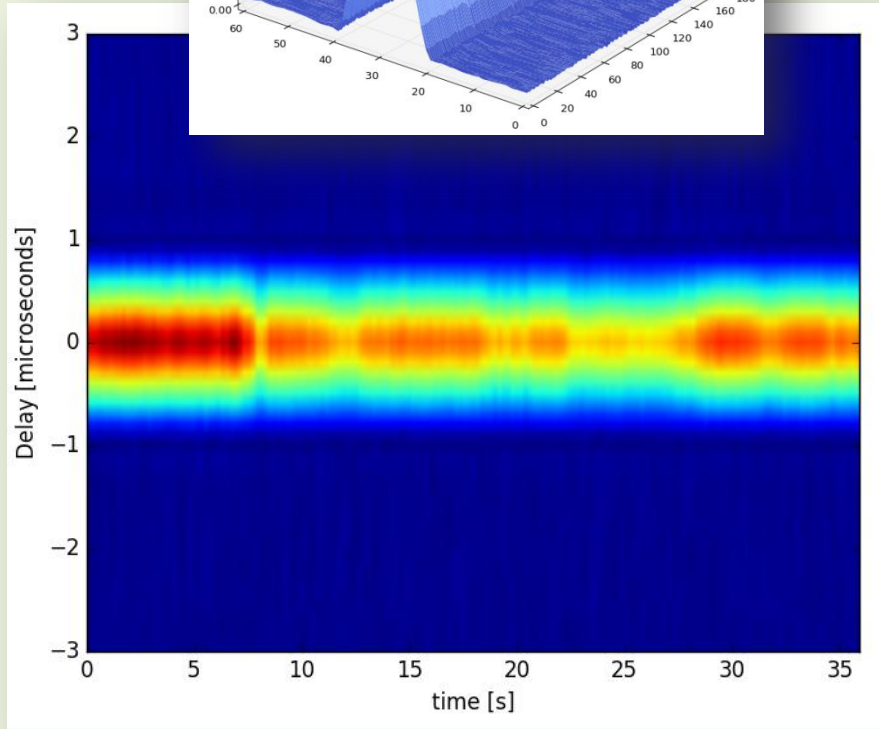
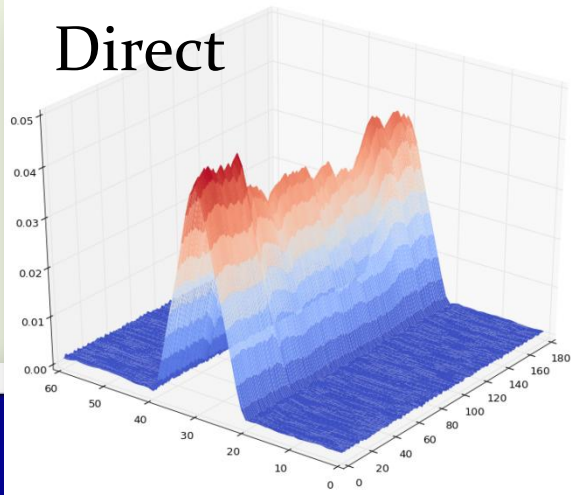
Nadir-looking antenna (Cobham DS1563)
 cross-polarization isolation: Left: LHCP
 Port, Right: RHCP Port. The radial scale
 is the incidence angle.

ANALYSIS OF GNSS-R DATA

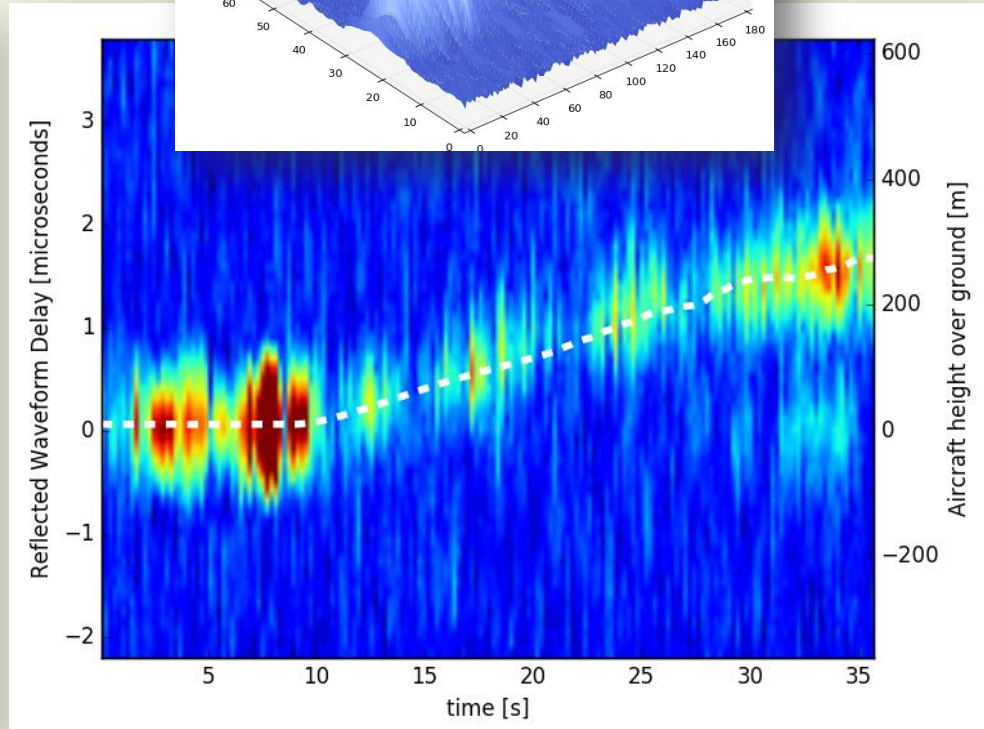
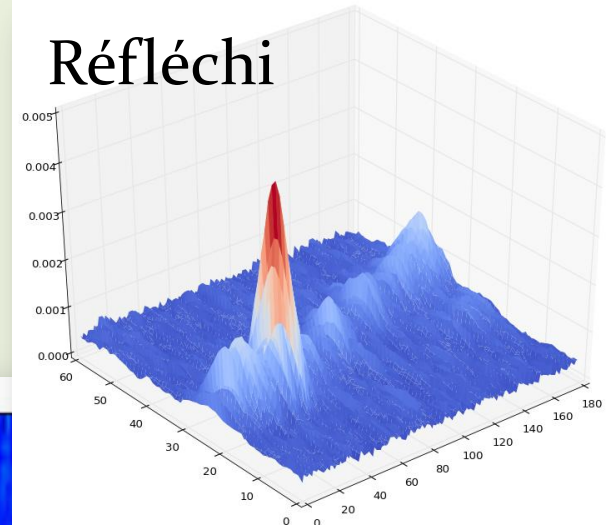


WAVEFORMS ESTIMATION

Direct

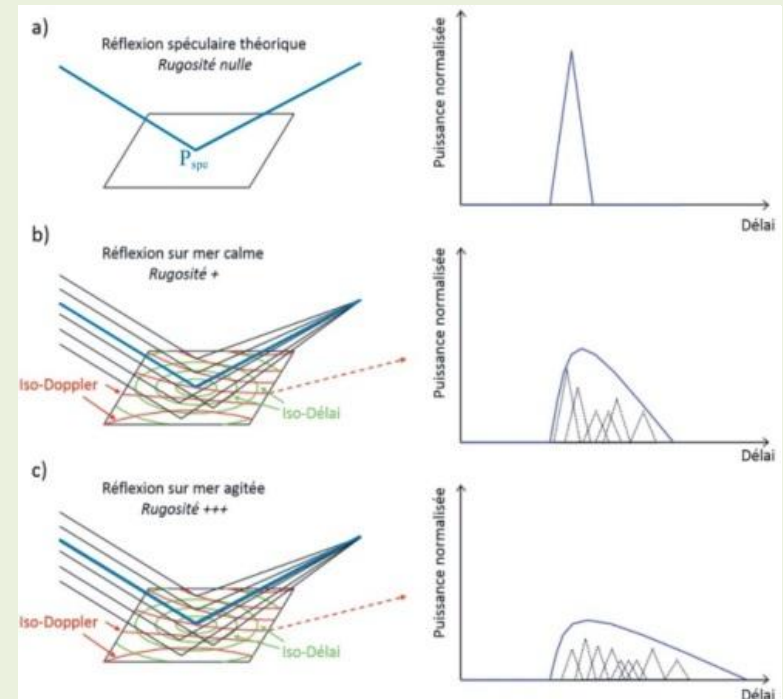
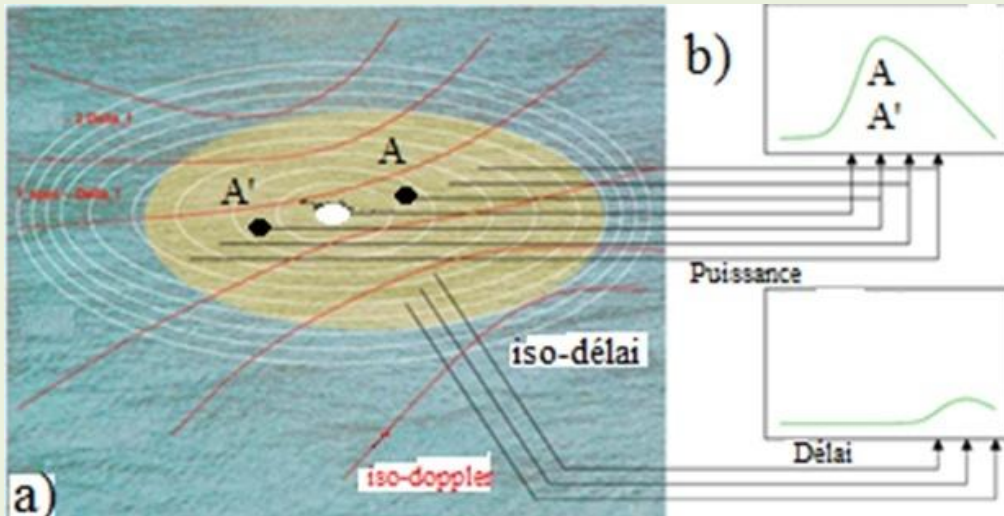


Réfléchi



COHERENT AND INCOHERENT SCATTERING

- The more a surface is rough, the more points that are further away from the specular point will contribute to the signal received by the receiver.
- The active area of scatter, which contributes to the reflected signal, is known as the glistening zone.



$$\Delta\tau(x, y) = \tau(x, y) - \tau_{spec} \quad \Delta\rho = \Delta\tau \cdot C$$

Points with the same delay are iso-delay ellipses.

$$f_d(\vec{\rho}) = \frac{(\vec{v}_t \cdot \hat{m} \vec{\rho}) + (\vec{v}_r \cdot \hat{n} \vec{\rho})}{\lambda}$$

Points with an identical Doppler shift describe hyperbolas said to be iso-Doppler lines;

OTHER OBSERVABLES (WAVEFORM ANALYSIS)

SURFACE REFLECTIVITY (COHERENT COMPONENT)

REFLECTIVITY

the ratio of direct and reflected waveforms, in the case of signals that are not affected by thermal noise

$$\Gamma'_{pq} = \left| \left\langle \frac{Y_{r,q}(\Delta\tau, f)}{Y_{d,p}(0, f)} \right\rangle \right|^2$$

INTERFEROMETRIC COMPLEX FIELD

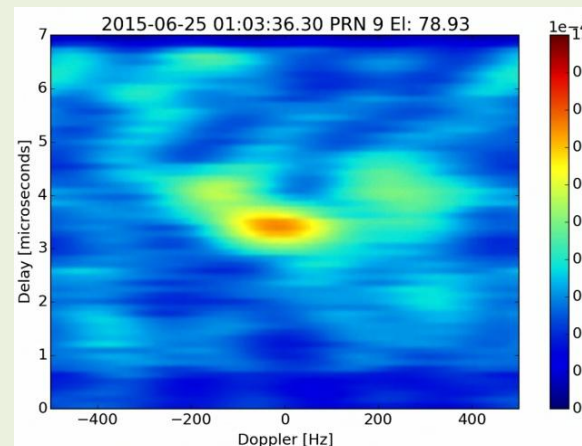
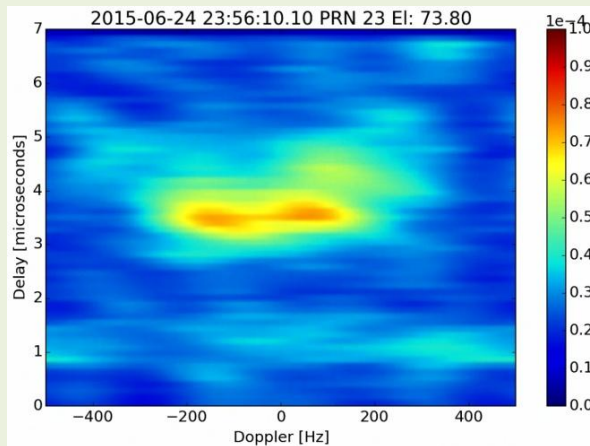
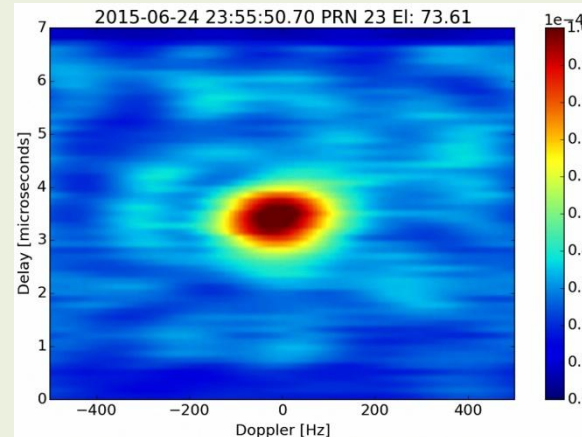
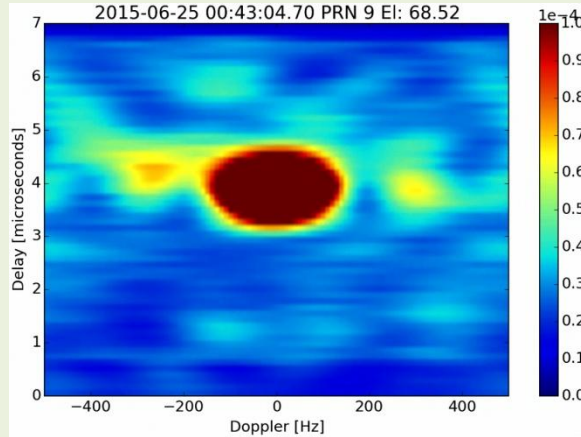
time series of the relative maxima of reflected waveforms over those of direct waveforms:

$$ICF(t) = \frac{Y_{r,q}(t, \Delta\tau, f)}{Y_{d,p}(t, 0, f)} = \frac{R(t)}{D(t)} = \frac{r(t)}{d(t)} e^{-i(\phi_r(t) - \phi_d(t))}$$

DDM: DELAY DOPPLER MAP

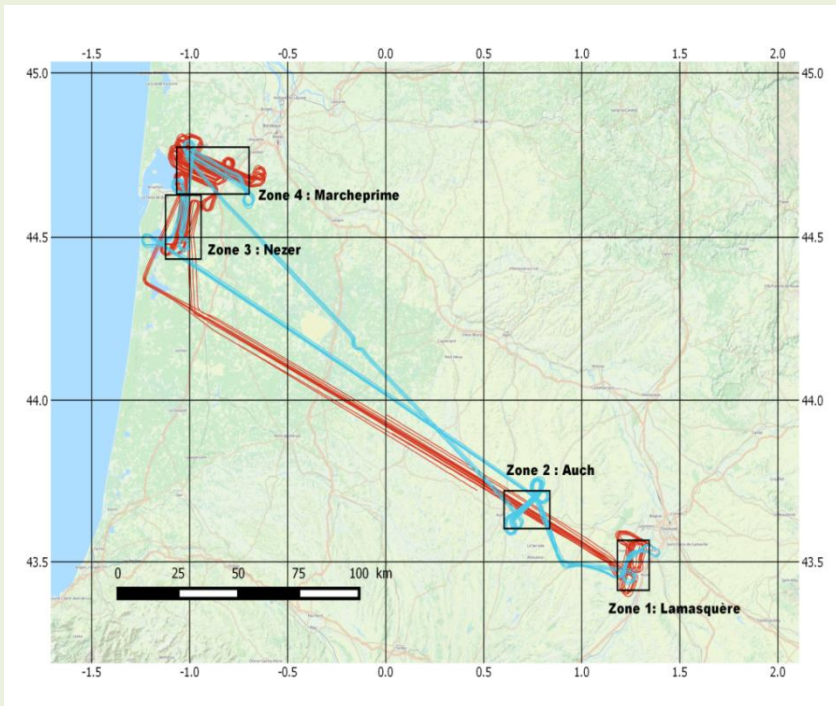
DDM

$$\langle |Y(\tau, f)|^2 \rangle = \frac{T_i^2 P_t G_t \lambda^2}{(4\pi)^3} \iint_A \frac{G_r(\vec{\rho})}{R_0^2(\vec{\rho}) R^2(\vec{\rho})} \sigma_{pq}^0 \chi^2(\vec{\rho}, \delta\tau, \delta f) d\vec{\rho}$$



Delay Doppler Maps of reflected signals over: (a) water cover, (b) bare soil (c) developed corn field (d) Pine tree forest (age 15 years approx.). Aircraft altitude is about 600 meters, coherent integration time is 5ms and incoherent averaging time is 200ms.

GLORI MEASUREMENTS



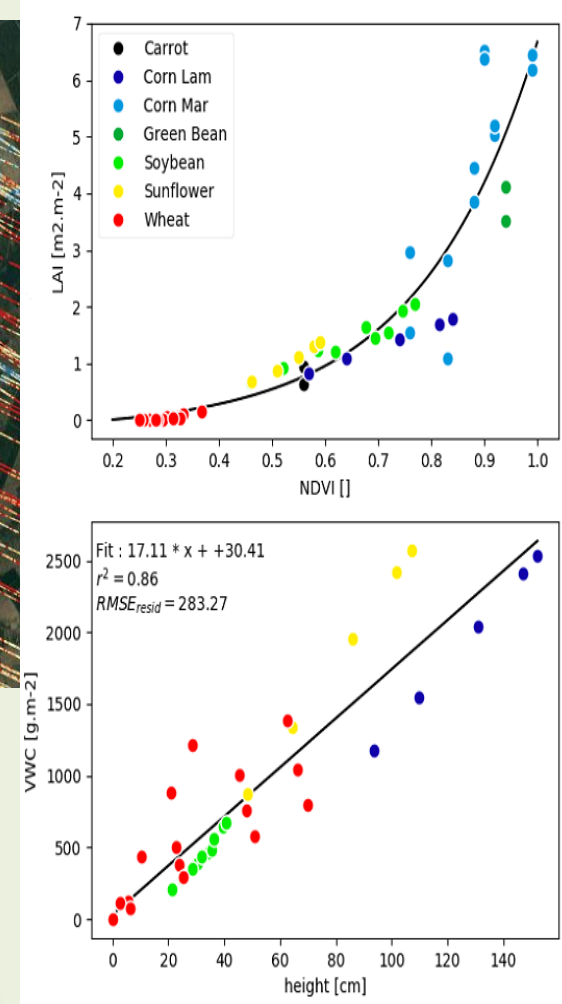
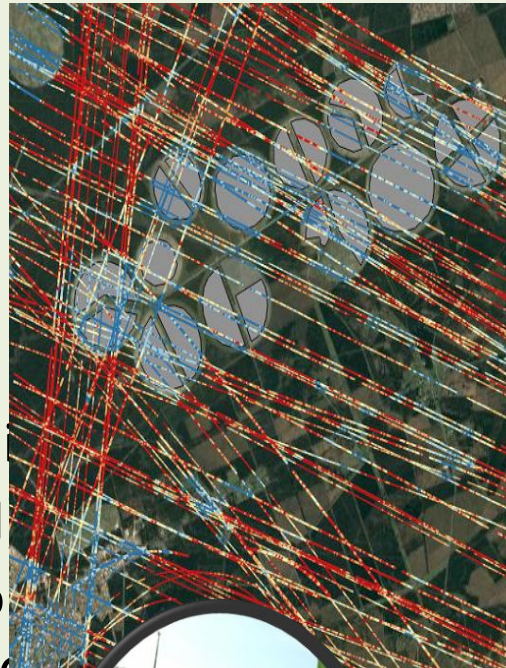
GLORI flights'2015 over south west (agricultural sites, Landes forest)

GLORI reflectivity over different land uses
 → Highest reflectivity for water covers

$$\Gamma'_{pq} = \left| \left\langle \frac{Y_{r,q}(\Delta\tau, f)}{Y_{d,p}(0, f)} \right\rangle \right|^2$$

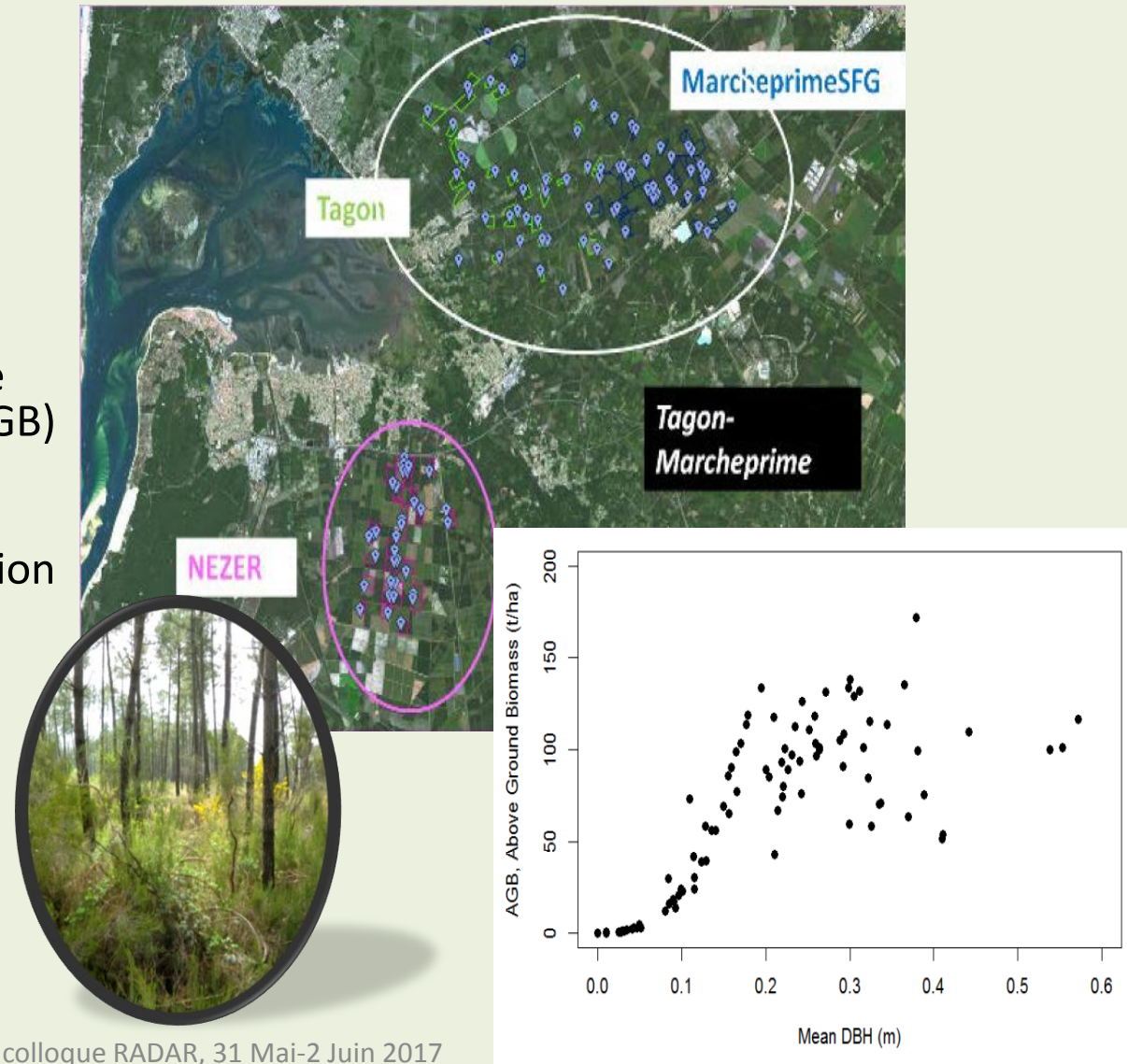
In situ ground truth dataset – Agricultural

- Parameters:
 - Soil moisture
 - Roughness
 - vegetation cover height
 - Leaf Area Index (LAI)
 - vegetation water content
 - NDVI from optical EO
- Extent
 - 3 areas
 - 30 fields
 - Several crop types

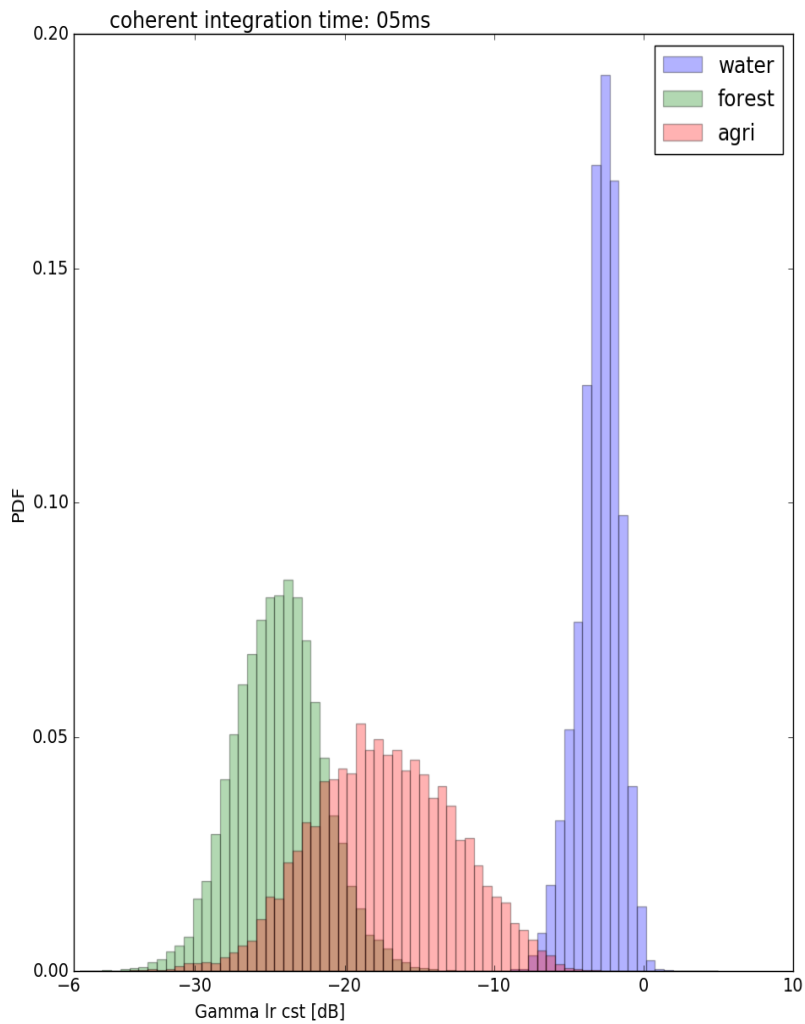


In situ ground truth dataset – Forest

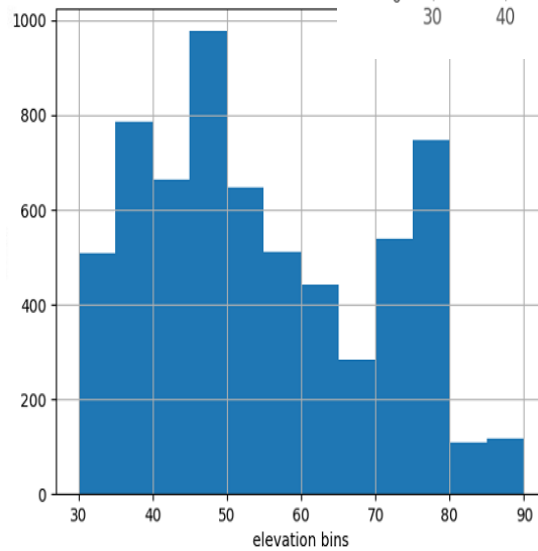
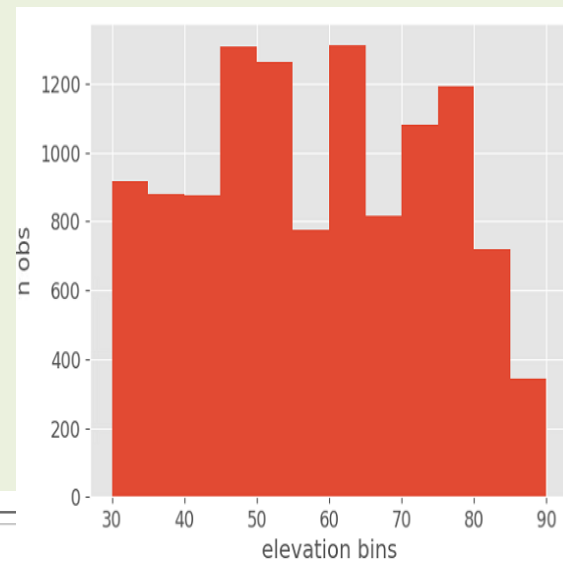
- Parameters:
 - Age
 - Diameter (DBH)
 - Height
 - Density
 - Estimation of Above Ground Biomass (AGB) from allometric equations
 - Qualitative description of ground cover
- Extent
 - 3 areas
 - 100+ stands
 - Biomass up to 150 t/Ha



Distribution des mesures

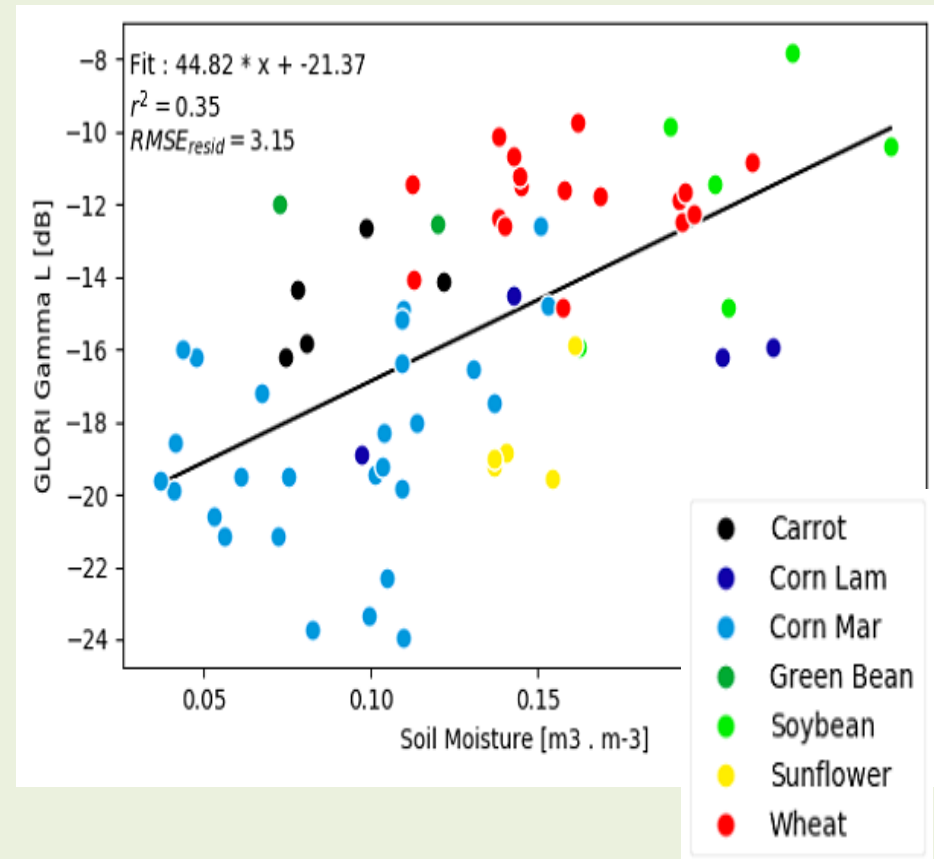
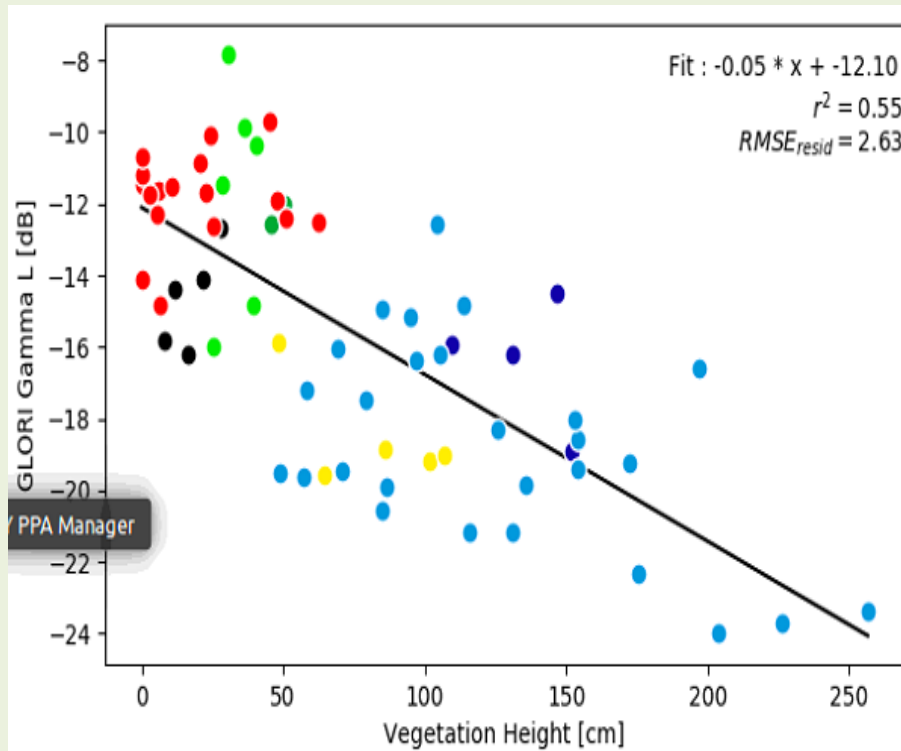


Forests



Agricultural

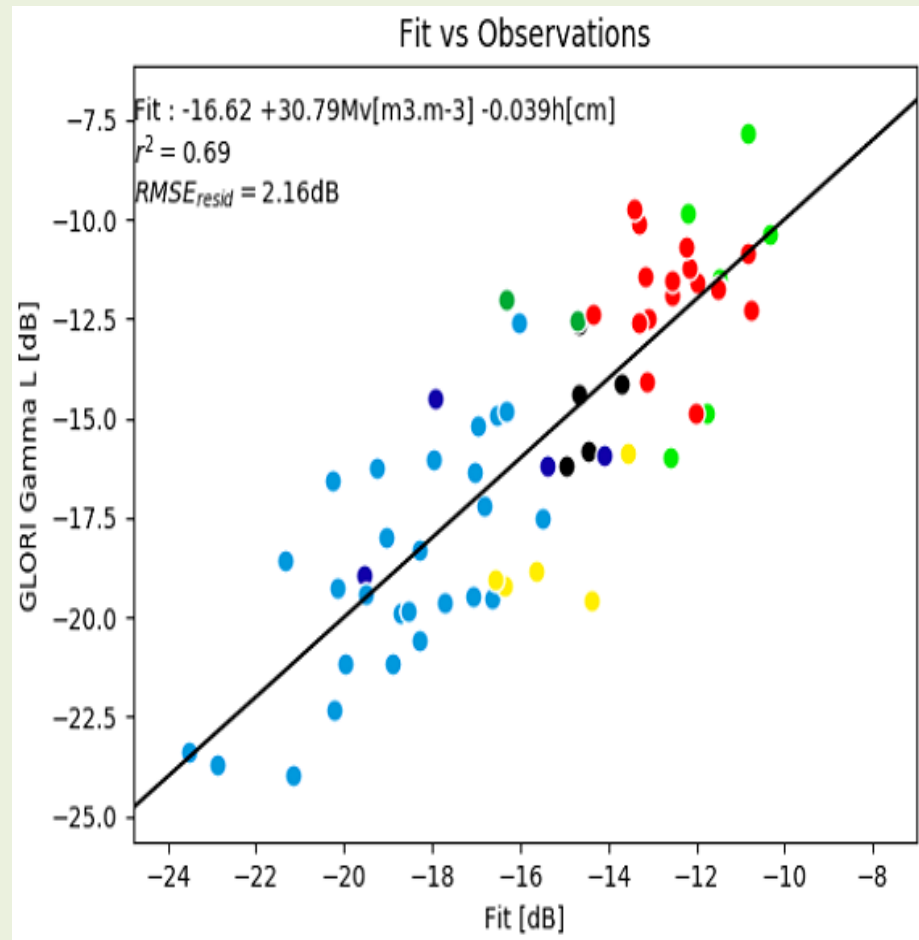
Results, Agricultural areas, LHCP



All elevations (30-90) -> Sensitivity to vegetation height and soil moisture

Results, Agricultural areas, LHCP

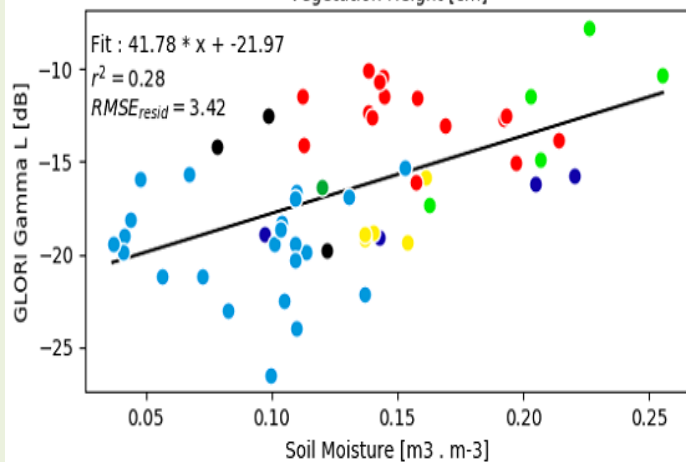
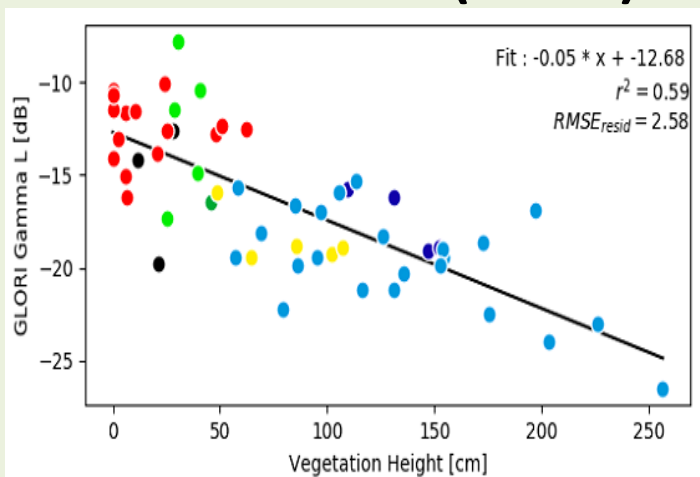
$$\Gamma_p(\theta) = \Gamma_p^{soil}(\theta) \cdot e^{-2 \cdot \tau_p^{canopy} / \cos \theta} \cdot (1 - \omega_p^{canopy})^2$$



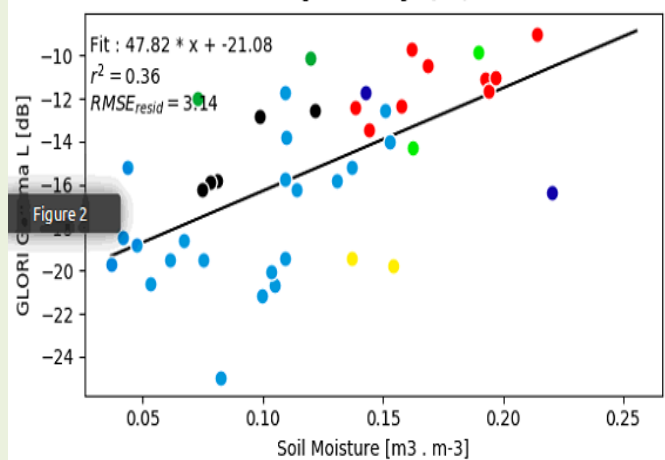
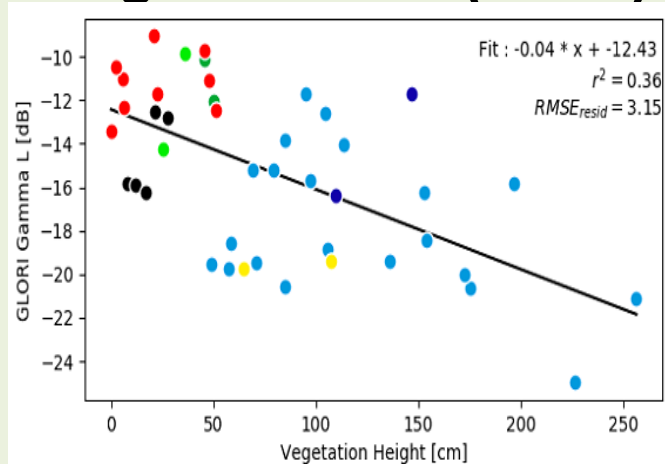
Multi linear fit: Soil Moisture and vegetation Height : $r^2=0.7$

Results, Agricultural areas, LHCP

Low elevation (30-60)



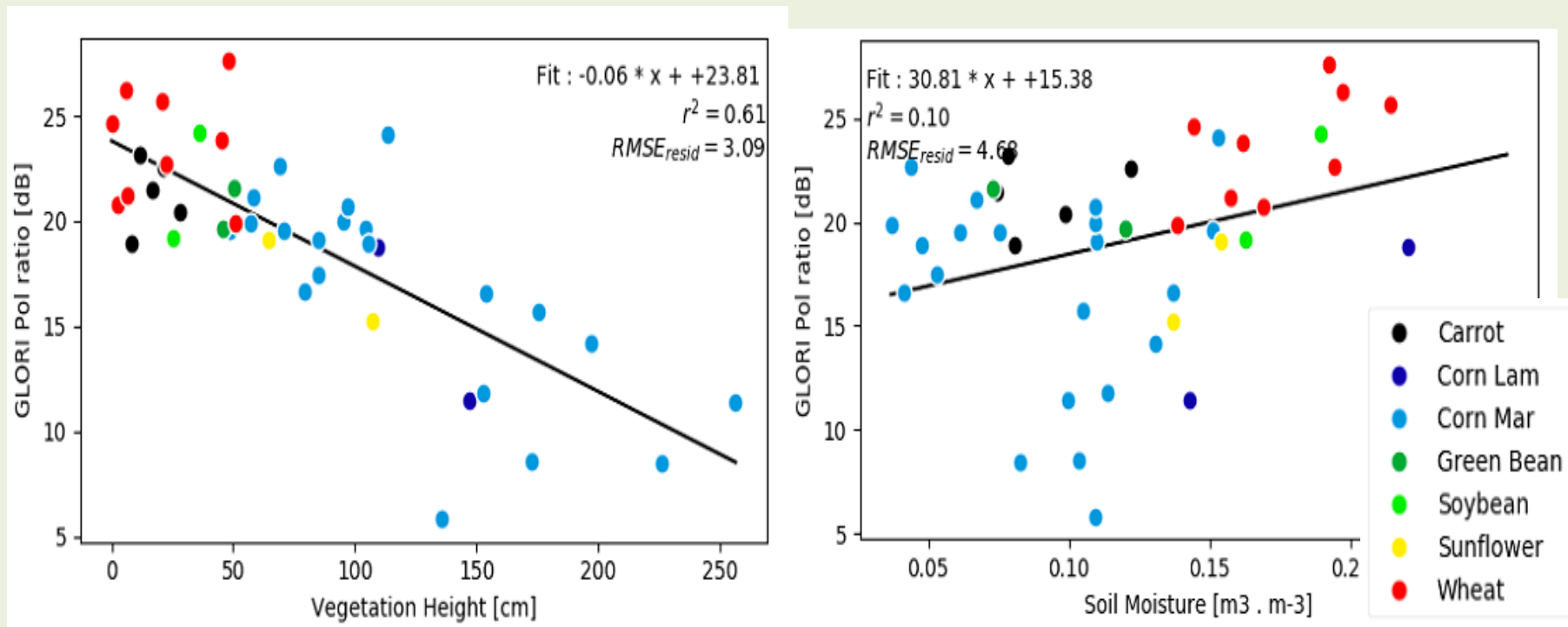
High elevation (60-90)



Veg +, SM - colloque RADAR, 31 Mai-2 Juin 2017

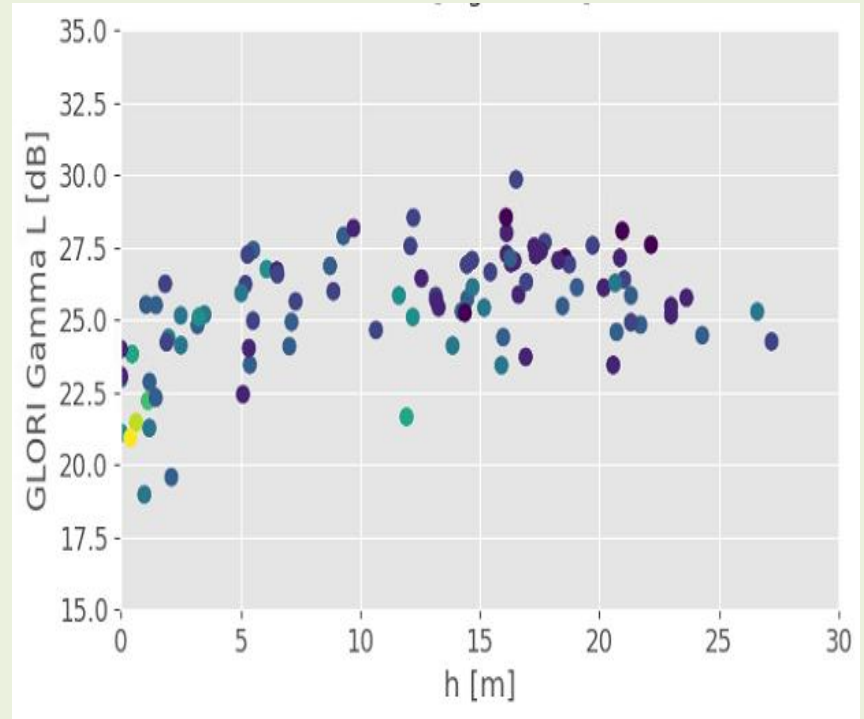
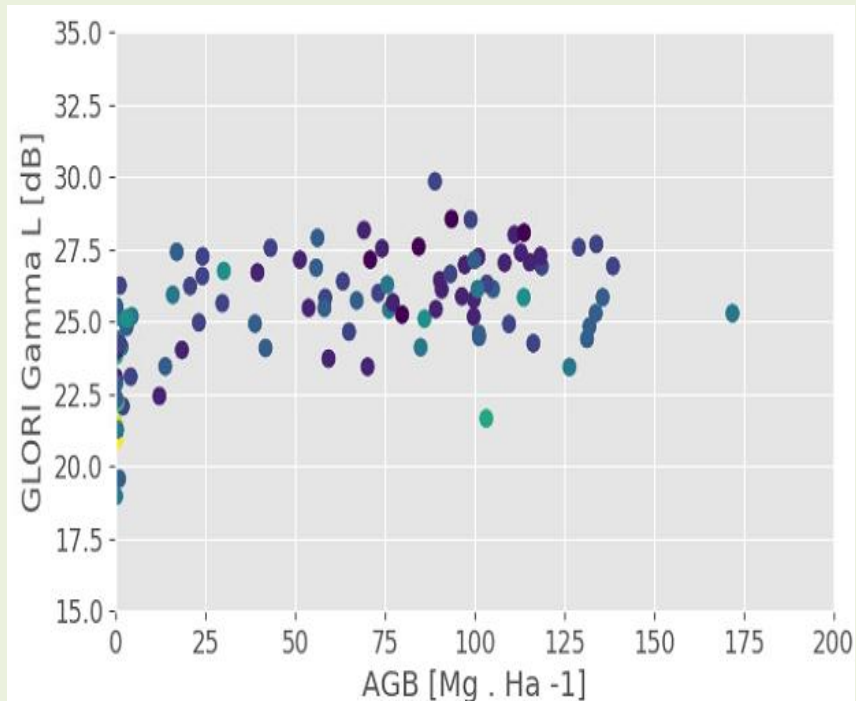
Veg -, SM +

Results, Agricultural areas, polar ratio



Only improvement: correlation with vegetation height at high elevation angle (60-90), no improvement for soil moisture.

Preliminary results, Forest areas



Saturation after 50 t/Ha or 10m. Effect of cover?



Vs.



« Bistatic radars using GNSS signals of opportunity offers a great potential for earth observation due to their temporal and geophysical availability, their self calibrated nature, and the size and power requirements for most of the GNSS-R systems. They have just arrived, but are here to stay »

A. Camps

Thank you for your attention!

Remerciements au TOSCA/CNES